STEM CELLS AND DEVELOPMENT
Volume 28, Number 15, 2019

DOI: 10.1089/scd.2019.0125

Histone Methylation Mechanisms Modulate the Inflammatory Response of Periodontal Ligament Progenitors

Marybeth Francis,[1,2] Mirali Pandya,[1] Gokul Gopinathan,[1] Huling Lyu,[3] Wei Ma,[4] Deborah Foyle,[1] Salvadore Nares,[5] and Xianghong Luan[1]

Inflammatory conditions affect periodontal ligament (PDL) homeostasis and diminish its regenerative capacity. The complexity of biological activities during an inflammatory response depends on genetic and epigenetic mechanisms. To characterize the epigenetic changes in response to periodontal pathogens we have focused on histone lysine methylation as a relatively stable chromatin modification involved in the epigenetic activation and repression of transcription and a prime candidate mechanism responsible for the exacerbated and prolonged response of periodontal cells and tissues to dental plaque biofilm. To determine the effect of inflammatory conditions on histone methylation profiles, related gene expression and cellular functions of human periodontal ligament (hPDL) progenitor cells, a hPDL cell culture system was subjected to bacterial cell wall toxin exposure [lipopolysaccharide (LPS)]. Chromatin immunoprecipitation-on-chip analysis revealed that healthy PDL cells featured high enrichment levels for the active H3K4me3 mark at *COL1A1*, *COL3*, and *RUNX2* gene promoters, whereas there were high occupancy levels for the repressive H3K27me3 marks at *DEFA4, CCL5*, and *IL-1β* gene promoters. In response to LPS, H3K27me3 enrichment increased on extracellular matrix and osteogenesis lineage gene promoters, whereas H3K4me3 enrichment increased on the promoters of inflammatory response genes, suggestive of an involvement of epigenetic mechanisms in periodontal lineage differentiation and in the coordination of the periodontal inflammatory response. On a gene expression level, LPS treatment downregulated *COL1A1*, *COL3A1*, and *RUNX2* expression and upregulated *CCL5*, *DEFA4*, and *IL-1β* gene expression. LPS also greatly affected PDL progenitor function, including a reduction in proliferation and differentiation potential and an increase in cell migration capacity. Confirming the role of epigenetic mechanisms in periodontal inflammatory conditions, our studies highlight the significant role of histone methylation mechanisms and modification enzymes in the inflammatory response to LPS bacterial cell wall toxins and periodontal stem cell function.

Keywords: periodontal ligament, inflammation, extracellular matrix genes, epigenetic regulation

Introduction

The periodontal ligament (PDL) is a unique, nonmineralized connective tissue localized between tooth root cementum and alveolar bone. The major functions of the PDL include tooth support, homeostasis, and protection of the underlying tissues from pathogens in the oral cavity and tissue repair. The PDL contains heterogeneous cell populations including PDL stem cells (PDLSCs) [1,2]. Periodontal stem cells are mesenchymal progenitor cells that have the ability to proliferate and differentiate and to participate in cementum, alveolar bone, and PDL regeneration after injury, periodontal therapy, tooth transplantation, and/or replantation, and orthodontic tooth movement [3–6]. Compared with their neural crest precursors, PDL progenitors are committed progenitors characterized by the expression of collagen and RUNX2 genes as periodontal lineage marker genes [7].

Inflammation in the periodontium results from the host response to the oral biofilm and is the major cause of periodontal disease. If untreated and progressive, periodontal disease has deleterious consequences for the health of the dentition, including PDL destruction, alveolar bone loss, and ultimately tooth loss. On a biological level, inflammatory conditions diminish PDL homeostasis and its tissue regeneration capacity [8]. Although PDLSCs are present both in healthy and in diseased PDL tissues, inflammatory conditions

[1]Department of Periodontics, Center for Craniofacial Research and Diagnosis, Texas A&M College of Dentistry, Dallas, Texas.
[2]Department of Oral Biology, UIC College of Dentistry, Chicago, Illinois.
[3]Key Laboratory of Oral Medicine, Guangzhou Institute of Oral Disease, Stomatological Hospital of Guangzhou Medical University, Guangzhou, China.
[4]Department of Stomatology, The Fourth Affiliated Hospital, Harbin Medical University, Harbin, China.
[5]Department of Periodontics, UIC College of Dentistry, Chicago, Illinois.

affect the number, proliferation, and distribution of periodontal progenitors; enhance their migratory capacity; and impair their osteogenic potential [9–13].

The onset of periodontal disease is characterized by an inflammatory response to the lipopolysaccharide (LPS) from the cell walls of the gram-negative bacteria that constitute the majority of the pathogenic periodontal microflora [14]. In response to LPS, PDL cells produce proinflammatory cytokines, chemokines, and matrix metalloproteinases, which are responsible for inflammatory infiltration and tissue destruction in the periodontium [15–17]. LPS also modifies the differentiation potential of PDLSCs [18]. From a mechanistic perspective, LPS is a ligand of Toll ligand receptors, and activates nuclear factor kappa B (NF-κB) signaling through the toll-like receptor (TLR) pathway [19].

Previous studies have demonstrated that epigenetic regulation of gene expression affects the differentiation and function of mesenchymal stem cells (MSCs) [20–23]. Several epigenetic mechanisms including histone modification, DNA methylation, and nuclear positioning control chromatin structure and regulate gene expression by modulating the accessibility for transcription factors to interact with the promoters and enhancers of the regulated genes [24]. Among these mechanisms, histone methylation is involved in both activation and repression of gene expression. Trimethylation of histone H3 at lysine-4, -36, and -79 (H3K4me3, H3K36me3, and H3K79me3) results in active marks, whereas trimethylation of H3 at lysine-9 and -27 (H3K9me3 and H3K27me3) indicates repressive marks [25,26]. Histone methylation studies in embryonic and other stem cells have identified regions that were marked for both H3K27me3 and H3K4me3 [27–29]. Promoter regions that are bivalently marked for both H3K4me3 and H3K27me3 are indicative of genes that are poised for transcription and may be further methylated for repression or for activation of gene expression in MSCs [30].

In previous studies we have demonstrated that odontogenic lineage specification and progenitor differentiation are regulated by changes in histone methylation [31]. Furthermore, histone methylation is also affected by inflammation [32]. In this study, we have hypothesized that inflammation as it occurs during periodontal disease affects periodontal progenitor cell function by dysregulating gene expression of periodontal matrix genes and inflammatory response genes. To characterize the epigenetic response to periodontal pathogens in periodontal stem cells, we have analyzed H3K4 and H3K27 histone trimethylation in response to LPS exposure, and correlated our findings with data related to matrix protein and inflammatory response gene expression, cell function, and differentiation after LPS treatment.

Materials and Methods

Cell culture

PDL progenitor cells (PDLSCs) were isolated from human extracted third molars, and maintained in Dulbecco's modified Eagle's medium (DMEM; Gibco BRL, Gaithersburg, MD) supplemented with 10% fetal bovine serum (FBS; Atlanta Biologicals, Lawrenceville, GA), 100 U/mL penicillin, 100 μg/mL streptomycin, and 25 ng/mL amphotericin B in a 5% CO_2 atmosphere at 37°C. This procedure followed the human subject regulations of Texas A&M University and University of Illinois. Inflammatory conditions were mimicked by adding 10 μg/mL Pg-LPS (InvivoGene, San Diego, CA) or *Escherichia coli* LPS (strain 0111:B4; Sigma-Aldrich Chemical, St Louis, MO) to the culture medium. To study the effects of LPS on osteogenic differentiation, human periodontal ligament stem cells (hPDLSCs) were subjected to a mineralization induction medium containing 10 nM dexamethasone, 50 μg/mL ascorbic acid, and 2 mM β-glycerophosphate and cultured for 14 or 28 days. Upon terminating the culture, cells were subjected to alkaline phosphatase (ALP) activity assays or alizarin red staining.

Chromatin immunoprecipitation-on-chip analysis

Sample preparation. PDL cells grown on 150-mm plates were crosslinked with 1.1% formaldehyde at room temperature. The reaction was stopped with 125 mM glycine. Cells were harvested, and pooled cells were then aliquoted, flash frozen, and stored at −80°C. For chromatin immunoprecipitation (ChIP) assays, nuclei were prepared from 1×10^6 cells and resuspended in lysis buffer. After incubation on ice, nuclear lysates were sonicated to a size of 300 bp to 1 kb in a cup horn sonicator (Qsonica, Newton, CT). Sheared chromatin was centrifuged at 12,000 rpm and incubated overnight with 100 μL of DynaI beads (Invitrogen, Carlsbad, CA), prebound with 10 μg of antibody against each histone modification: histone H3 trimethyl K4 and histone H3 trimethyl K27 (ab8580, ab8898; Abcam, Cambridge, United Kingdom). An input fraction was kept aside for background normalization. Next, beads were separated on a magnetic stand and washed 5 times with RIPA buffer and once with 1 × Tris-EDTA buffer (TE). Bound protein–DNA complexes were eluted from the beads by incubating with the elution buffer at 65°C, followed by crosslink-reversal overnight at 65°C. DNA was purified by proteinase K digestion, phenol–chloroform extraction, and ethanol precipitation. The resulting pellet was resuspended in Tris buffer (pH 8.0). ChIP experiments were performed as triplicates.

ChIP-on-chip array. ChIP DNA quality and concentration were determined on a NanoDrop spectrophotometer. All samples were whole genome amplified. Dual-color labeling reactions were performed using the NimbleGen Dual-color labeling Protocol (ver 6.2). About 1 mg of IP and input DNA sample were labeled with Cy5 and Cy3, respectively. Labeled DNA was then purified and the labeling efficiency was determined by the NanoDrop spectrophotometer. Fifteen micrograms of the labeled immunoprecipitated DNA was pooled for hybridization with 15 μg of labeled input DNA placed on the 3X720K Roche Human ChIP-chip Promoter microarray and hybridized at 42°C for 20 h. The arrays represent 22,542 promoters based on Human genome 18 build (HG18) with a tiling of 3,200 bp upstream and 800 bp downstream to each transcription start site (TSS). Finally, the arrays were washed and scanned at a 2-mm resolution on a NimbleGen MS 200 Microarray Scanner. Data were processed through DEVA software using NimbleScan Software User's Guide (ver 2.6) and the Design files and genome annotations for HG18 Refseq promoters. A quality experimental metrics report was generated for each sample that met the guidelines set by Roche NimbleGen.

Raw data processing and gene annotation. Datasets corresponding to histone enrichment values in both immunoprecipitated and input samples were used to obtain Ratio.GFF files

and merged to get average values for histone modification enrichment. These files were converted to wiggle files for visualization in an integrative genomics viewer (IGV) genome browser [31]. Software was used to obtain significant peaks that were mapped to 5,000 bp upstream and 1,000 bp downstream of the nearest TSS to generate a peak report [31]. Promoter information was used for downstream analysis [31].

ChIP-polymerase chain reaction analysis

ChIP-polymerase chain reaction (PCR) assays were performed with control and LPS-challenged experimental groups. All DNA samples obtained from ChIP were diluted to a concentration of 2 ng/μL. Real-time quantitative PCR was performed on an ABI 7500 FAST machine with 4 ng of ChIP DNA, and the total input was used as an internal reference for normalization. Enrichment for beads alone was used as a negative control. Data presented for each primer pair were obtained after subtracting the values obtained from the corresponding negative controls. The primer sequences are given in Table 1.

Table 1. Human Chromatin Immunoprecipitation and Reverse Transcriptase-Polymerase Chain reaction Primer Sequences

Oligonucleotides for ChIP (human)		
Col1a1	Forward	TTGGGTGTGGCTGTAAGAGA
	Reverse	GGGATCTTTCATGGTTTCCA
Col3a1	Forward	TATTTCAGAAAGGGGCTGGA
	Reverse	AGTTGTTCCCTGCCCTTCA
Runx2	Forward	AGCAGTTTGCAACCAGACCT
	Reverse	TGGCTGGATTCCTTCTGTTT
CCL5	Forward	TGAGAGAGCAGTGAGGGAGA
	Reverse	GCATTGGCCGGTATCATAAG
IL-1β	Forward	AAACCTCTTCGAGGCACAAG
	Reverse	GGCAGAGAGACAGAGAGA CTCC
DefA4	Forward	TTGGCCTGGATGACCTAGAC
	Reverse	GCTCCCGAGTAAAGGATGTG
Oligonucleotides for real-time PCR analysis (human)		
Col1a1	Forward	CATCTCCCCTTCGTTTTTGA
	Reverse	CCAAATCCGATGTTTCTGCT
Col3a1	Forward	GATCAGGCCAGTGGAAATGT
	Reverse	GTGTGTTTCGTGCAACCATC
Runx2	Forward	GTGCCTAGGCGCATTTCA
	Reverse	GCTCTTCTTACTGAGAGT GGAAGG
CCL5	Forward	TGCCCACATCAAGGAGTATTT
	Reverse	CCAGACTTGCTGTCCCTCTC
IL-1β	Forward	AGTACCTGAGCTCGCCAGTG
	Reverse	CTGGAAGGAGCACTTCATCTG
DefA4	Forward	TTCCAGGTCATGGAGGAATC
	Reverse	CTTTCTTCGGCAGCATTTTC
GAPDH	Forward	ACAGTCAGCCGCATCTTCTT
	Reverse	ACGACCAAATCCGTTGACTC
β-actin	Forward	GATGAGATTGGCATGGCTT
	Reverse	CACCTTCACCGTTCCAGTTT

ChIP, chromatin immunoprecipitation; PCR, polymerase chain reaction.

ALP assay, alizarin red staining, and light microscopy

To determine ALP activity, control and LPS-treated cells were washed and stained with ALP substrate (Roche Diagnostic, Indianapolis, IN). To determine mineralization potential, mineral deposits were detected after fixing with cold methanol and staining with 1% alizarin red solution. Phase-contrast images of control and LPS-treated hPDL cells were obtained using a Leica inverted microscope.

Colony-forming assay

Colony-forming assays were performed using hPDLSCs. Cells were cultured at a density of 10^4 per well in 6-well culture plate. After 7 days of culture, the cells were fixed with 4% buffered formaldehyde and then stained with 0.1% toluidine blue.

MTT cell proliferation assay

Human PDL cells were cultured in 96-well plates for 1–4 days. Before culture termination, cells were incubated in MTT solution (2 mg/mL of MTT in DMEM with 2% FBS) for 4 h. The MTT stained cells were lysed in HCl/isopropanol, and the absorbance was detected at 570 nm with background subtraction at 630 nm.

Cell migration assay

LPS was added into the culture medium in the lower chamber. The hPDL cells were seeded into each insert and allowed to migrate to the underside of the membrane for 24 h. BSA treatment was used as a control. The cultured cells were washed with phosphate-buffered saline (PBS) and cultured in growth medium. The nonmigrated cells on the upper surface of the membrane were removed and the migratory cells attached to the lower surface were stained with 4′ 6-diamidino-2-phenylindole (DAPI). The average number of migrated cells per field was counted using a Leica DMRX fluorescent microscope.

Cellular motility assay

The hPDL cells were grown to confluence on culture plate. A linear scratch was made using a sterile 200 μL pipette tip and the wells were washed 3 times with PBS. Six hours after the scratch, 10 μg/mL LPS were added to the cell cultures for 24 h. The remaining wound area was measured using ImageJ software [33].

In vivo subcutaneous implantation experiments

Twenty microliters of LPS solution (10 μg/mL) or 20 μL of PBS was applied to a collagen sponge (2 × 2 × 2 mm) and incubated at 4°C overnight to coat the scaffold surface, and then lyophilized [34]. The collagen sponges were mixed with hPDL cells and incubated at 37°C for 3 h [34]. The collagen sponges were implanted into the back of nude mice below the subcutis. The mice were killed 4 weeks after implantation and the implants were dissected and prepared for paraffin embedding histological examination [34]. This study followed the protocols approved by the Institutional Animal Care and Use Committees of Texas A&M University and University of Illinois.

Histological staining

Implants were deparaffinized, rehydrated in a descending ethanol series, and rinsed in deionized water. For hematoxylin and eosin staining, sections were dipped in hematoxylin for 5 min, placed in PBS for 5 min, dipped in eosin for 1 min, dehydrated in an ascending ethanol series, and finally cleared in xylene. Sections were mounted with cover slips using Permount (Fischer Scientific, Hampton, NH). Masson's Trichrome staining was used to mark collagen fibers. For this procedure, deparaffinized and rehydrated sections were refixed in Bouin's solution for 1 h at 56°C, stained in Weigert's iron hematoxylin working solution for 10 min, in Biebrich scarlet-acid fuchsin solution for 15 min, and then transferred to aniline blue solution and stained for 10 min. Collagen stained blue, nucleus stained black and muscle, cytoplasm, and keratin stained red. To determine the mineralization, the sections of undecalcified implants were stained with alizarin red as described previously.

RNA extraction and reverse transcriptase (RT) real-time PCR

Total RNAs were isolated from human PDL cells using the RNeasy® Plus Mini Kit according to the manufacturer's instructions (Qiagen, Hildin, Germany). Two micrograms of total extracted RNA was applied toward cDNA generation with the Sprint RT Complete Kit® (Clontech, Mountain View, CA). Real-time PCR was performed with sequence-specific primers, using SYBR green Master Mix and the ABI Prism 7000 Sequence detection system (Applied Biosystems, Carlsbad, CA). Reaction conditions were as follows: 2 min at 50°C (1 cycle), 10 min at 95°C (1 cycle), 15 s at 95°C, and

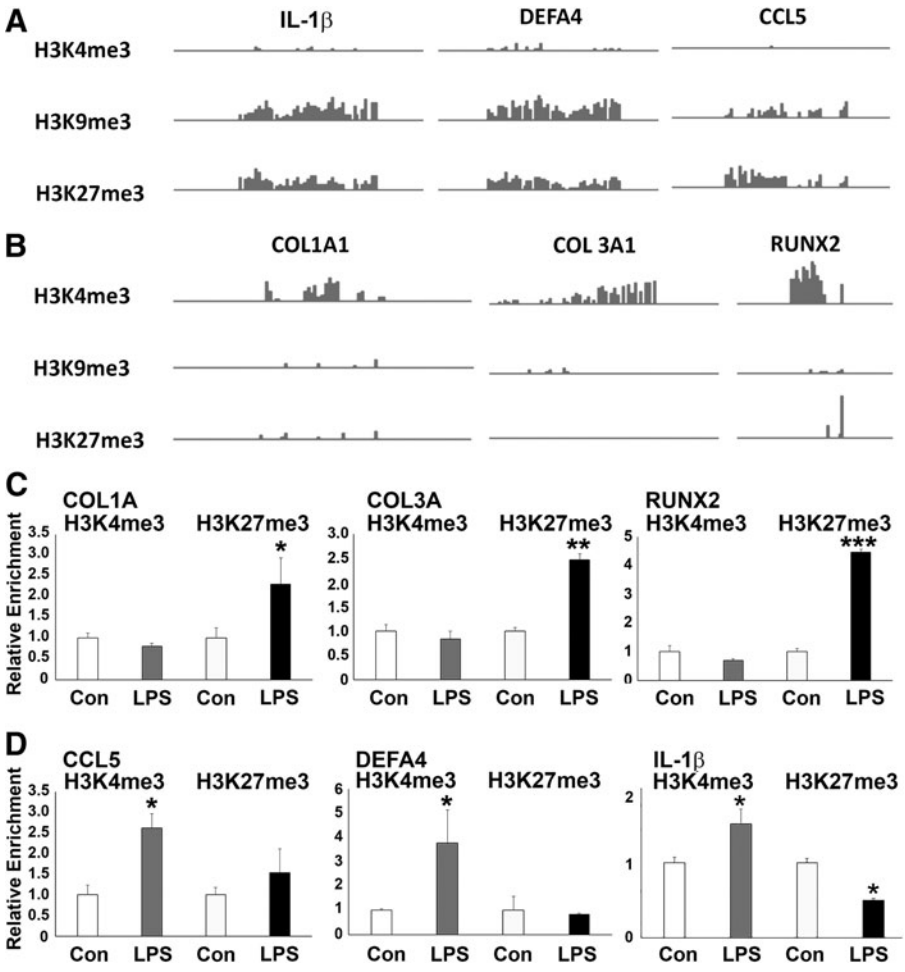

FIG. 1. ChIP-chip enrichment profiles of inflammatory and bone matrix genes in hPDL cells and comparison of histone modification patterns at osteogenic and inflammatory gene promoters after LPS treatment. **(A, B)** Representative view of histone enrichment profiles for select genes obtained using the IGV genome browser. Note the higher H3K9me3 and H3K27me3 enrichment levels at *IL-1β*, *DEFA4*, and *CCL5* promoters compared with the higher H3K4me3 enrichment levels at *COL1A1*, *COL3*, and *RUNX2* promoters in hPDL cells. **(C, D)** ChIP-PCR analysis of H3K4me3 and H3K27me3 enrichment on the *COL1A1*, *COL3*, *RUNX2*, *CCL5*, *DEFA4*, and *IL-1β* promoters in LPS-treated PDL cells compared with control cells. Representative graphs demonstrate relative enrichment compared with input DNA for H3K4me3 and H3K27me3. ChIP-qPCRs were performed at least 3 times with similar results. Statistical significance was determined by the unpaired Student's *t*-test with Welch's correction for unequal variances. *, **, *** represent a significant difference equivalent to the following *P*-values, $P < 0.05$, $P < 0.01$, $P < 0.001$. ChIP, chromatin immunoprecipitation; hPDL, human periodontal ligament; LPS, lipopolysaccharide; PCR, polymerase chain reaction.

1 min at 60°C (40 cycles). Samples were normalized to levels of β-actin or GAPDH. The analyses were performed in 96-well plate reactions with 2 reference gene wells and 2 target gene wells per sample. To quantify relative differences in mRNA expression, the comparative CT method (ΔΔCT) was used to determine relative quantity. Values were graphed as the mean expression level ± standard deviation.

Statistical analysis

Comparison of the results in each experimental group was performed using an unpaired Student's *t*-test with Welch's correction for unequal variances. One-way analysis of variance with Dunnett post hoc test was used to evaluate significant differences among experimental groups. All calculations were performed using GraphPad Prism 6.

Results

Epigenetic mechanisms controlled the commitment of hPDLSCs

ChIP-on-chip analysis revealed the occupancy patterns of histone methylation marks H3K4me3, H3K9me3, and H3K27me3 on the promoter regions of the matrix proteins *COL1A1*, *COL3A1*, and the osteogenesis master gene *RUNX2*, as well as the inflammation-related genes *CCL5, DEFA4*, and *IL-1β*. The active mark H3K4me3 displayed higher enrichment levels at *COL1A1*, *COL3A1*, and *RUNX2* genes (Fig. 1A), whereas the repressive marks H3K9me3 and H3K27me3 demonstrated higher occupancy levels at *CCL5*, *DEFA4*, and *IL-1β* genes in hPDLSCs (Fig. 1B).

LPS increased H3K27me3 occupancy on the promoter regions of osteogenic genes and increased H3K4me3 occupancy on inflammatory response genes

In our hPDL cell culture system, inflammatory condition was mimicked by adding LPS to culture medium. Upon LPS stimulation, the occupancy of the repressive mark H3K27me3 was dramatically enhanced, whereas the enrichment of the active mark H3K4me3 was reduced on the promoters of *COL1A1*, *COL3*, and *RUNX2* genes (Fig. 1C). In contrast, the inflammatory response genes *CCL5*, *DEFA4*, and *IL-1β* were predominantly marked with the active H3K4me3 mark, whereas there was no significant change in the occupancy of the repressive H3K27me3 mark on the promoters of *CCL5* and *DEFA4* genes in PDL-treated hPDLSCs compared with the control group (Fig. 1D).

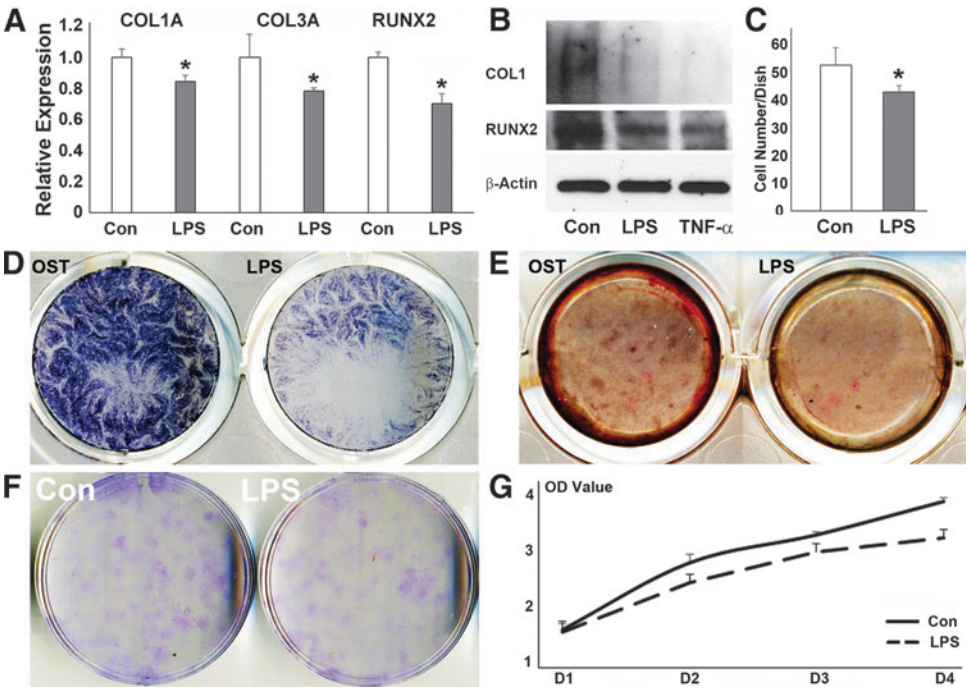

FIG. 2. Effects of LPS challenge on the expression of osteogenesis-related genes and osteogenic differentiation of hPDL cells. **(A)** Relative mRNA expression of *COL1A1*, *COL3*, and *RUNX2* by RT-qPCR. The relative expression levels of each gene in the LPS treatment group was calculated compared with the control group. Values were graphed as the mean expression level ± standard deviation. **(B)** Western blot of COL1A1 and RUNX2 protein expression in periodontal progenitors treated with PBS control, LPS, or TNF-α. β-actin was used as an internal control. **(C, F)** Effect of LPS exposure on cell growth and colony formation as revealed by colony formation assay and cell colony quantification. **(D)** Effect of LPS challenge on PDL cell function cultured in osteogenic medium for 7 days. Positive ALP staining was labeled *blue*. **(E)** Effect of LPS on mineral nodule formation. PDL cells were cultured in osteogenic medium for 21 days. Mineral nodules were visualized by alizarin red staining. **(G)** Effect of LPS challenge on cell proliferation as demonstrated by our MTT cell proliferation assay. Results were plotted as OD values. $^*p < 0.05$. ALP, alkaline phosphatase; OD, optical density; PDL, periodontal ligament; RT-qPCR, reverse transcriptase-quantitative polymerase chain reaction; TNF-α, tumor necrosis factor α.

Downregulation of osteogenesis-related gene expression and inhibition of osteogenic differentiation of hPDL cells after LPS challenge

In tandem to the increased occupancy of H3K27me3 on the promoters of *COL1A*, *COL3A*, and *RUNX2* genes, LPS challenge resulted in a significant decrease in the expression of *COL1A1* ($P < 0.001$), *COL3* ($P < 0.05$), and *RUNX2* ($P < 0.001$) compared with untreated control cells (Fig. 2A). Western blot analysis revealed that the expression of COL1A and RUNX2 proteins was reduced upon LPS challenge (Fig. 2B). LPS treatment also resulted in reduced ALP staining and alizarin red staining compared with control, indicative of an inhibition in mineralization (Fig. 2D, E). Colony-forming unit assays revealed that CFU-hPDL numbers were significantly reduced in LPS-treated hPDL cells versus controls ($P < 0.05$) (Fig. 2C, F). Finally, LPS treatment caused a gradual decrease in hPDL cell number in a time-dependent manner compared with the control group (Fig. 2G).

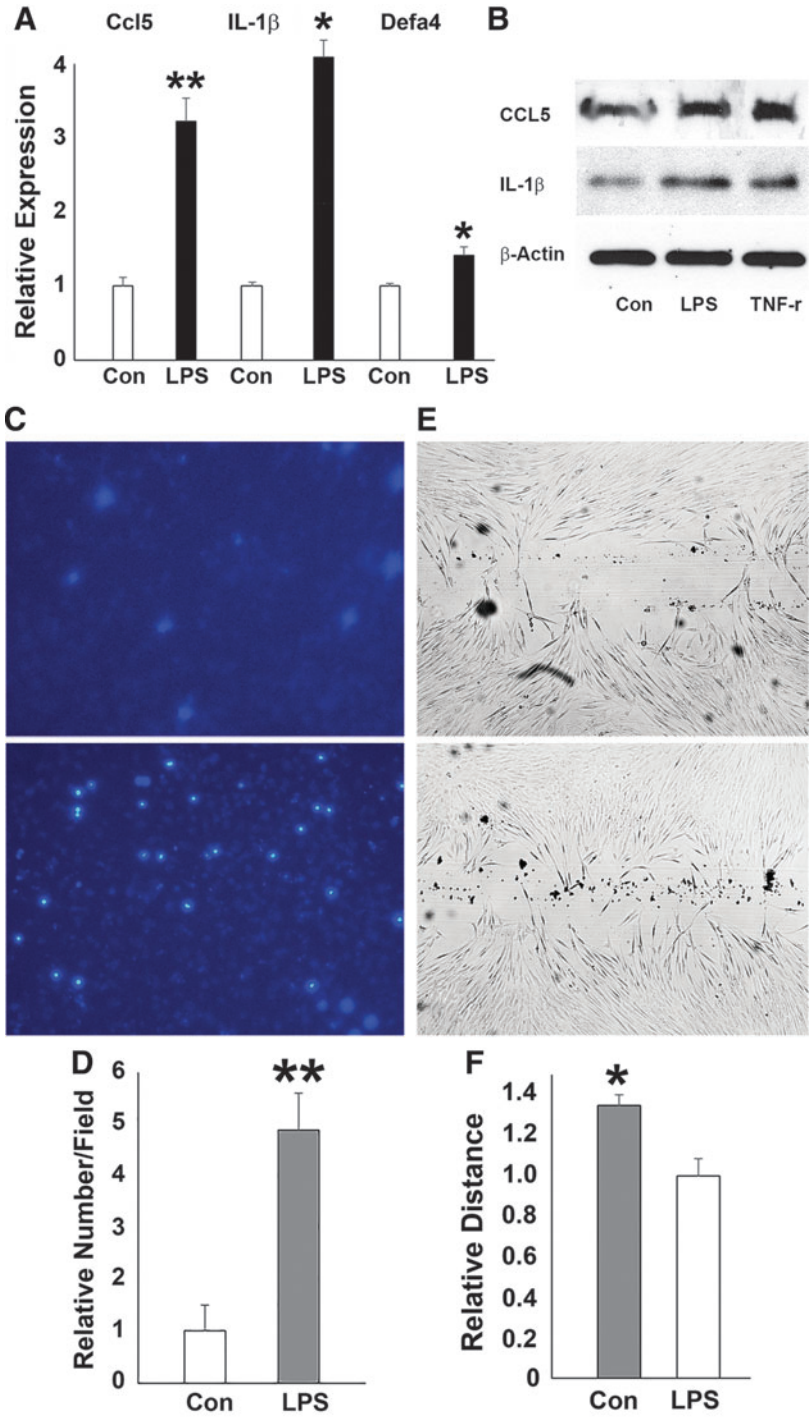

FIG. 3. Effects of LPS challenge on the expression of inflammatory response genes, and hPDL cell behavior. **(A)** Relative *IL-1β*, *DEFA4*, and *CCL5* mRNA expression in hPDL cells after LPS exposure as compared by RT-qPCR. **(B)** Western blotting of CCL-5 and IL-1β protein expression in periodontal progenitors treated with PBS control, LPS, or TNF-α. β-Actin was used as an internal control. **(C, D)** Transwell migration assay demonstrating the migration potential of LPS challenged cells. DAPI staining of hPDL nuclei on fluorescence blocking PET membranes to facilitate quantitation. The relative number of migrated PDL cells was 4.8 ($P < 0.05$) in the LPS-treated group compared with 1 in the control group. **(E, F)** Cell migration assessed using the scratch assay. In this assay, PDL cells were subjected to the scratch test. ImageJ was used to demonstrate that after 24 h LPS challenge, there was 30% more wound closure in the LPS treatment group ($P < 0.05$) compared with the control. PBS, phosphate-buffered saline; PET, polyethylene terephthalate. $*p < 0.05$; $**< 0.01$.

Upregulation of inflammatory response genes and changes in hPDL cell behavior after LPS challenge

In contrast to its effect on osteogenesis-related genes, LPS challenge resulted in increased expression of the inflammatory response genes *DEFA4*, *CCL5*, and *IL-1β* (Fig. 3A), matching our earlier data related to the enrichment of H3K4me3 mark on the promoters of *CCL5*, *DEFA4*, and *IL-1β* genes (Fig. 1). Western blot analysis demonstrated that the expression of CCL5 and IL-1β proteins was enhanced upon LPS challenge (Fig. 3B). LPS treatment also increased the number of DAPI-stained human PDL cells that migrated through the inserts in the transwell culture system (Fig. 3C). The relative number of migrated PDL cells was 4.8 times more ($P < 0.05$) in the LPS-treated group than that in the control group (Fig. 3D). In addition, our wound healing scratch assay demonstrated that after 24-h LPS challenge, there was 30% more wound closure than in non-LPS-treated controls ($P < 0.05$) (Fig. 3E, F).

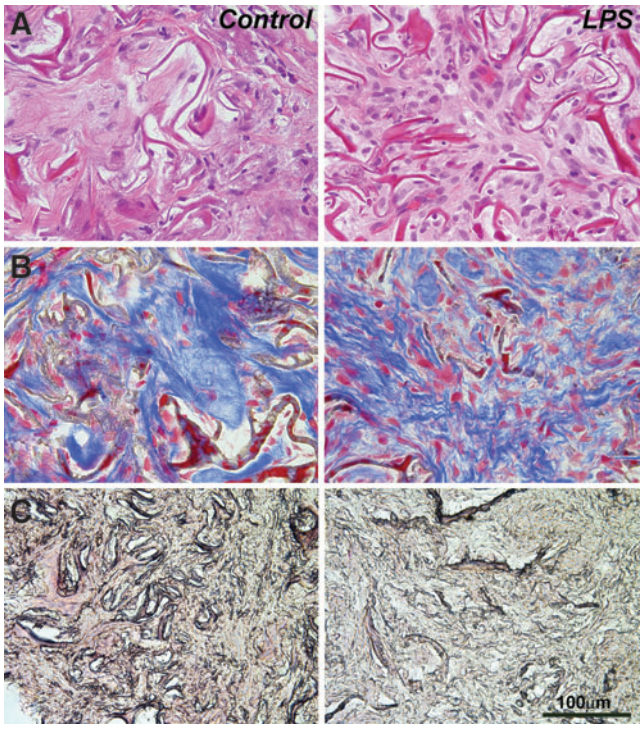

FIG. 4. Effect of LPS on extracellular matrix remodeling, cell migration, differentiation, and function in vivo. Collagen sponges were treated with PBS or LPS and subcutaneously implanted into nude mice for 4 weeks. **(A)** H&E staining of collagen sponge implants subjected to either PBS or LPS treatment. **(B)** Paraffin sections of collagen fibers in hPDL impregnated subcutaneous implants stained with Masson's trichrome. The micrographs are representative samples comparing a collagen sponge control treated with PBS versus the collagen sponge treated with LPS. **(C)** Representative paraffin sections of collagen sponge implants treated either with PBS or LPS and stained with alizarin red. H&E, hematoxylin and eosin.

LPS caused scaffold infiltration with migratory cells and extracellular matrix remodeling in subcutaneous implants

To determine the in vivo effect of LPS on the differentiation and function of PDLSCs in implanted tissue scaffolds, subcutaneous collagen sponge implants were treated either with LPS or PBS (physiological control), seeded with PDLSCs, harvested after 4 weeks, and prepared for paraffin sections (Fig. 4). Morphometry on 10 randomly selected sections revealed a 2.5-fold increase in cell number including inflammatory cells in LPS-treated implants compared with the PBS-treated control group (Fig. 4A). Using Masson's trichrome staining as a means to identify collagen fibers, the effect of LPS on collagen synthesis and remodeling of the subcutaneously implanted collagen scaffold was assessed. The extracellular matrix of the LPS-treated group consisted of short and thin collagen fibrils compared with the long and thick fibers and the dense fiber meshwork of the control group (Fig. 4B). Furthermore, LPS treatment decreased the amount of alizarin red staining compared with the control, implying decreased mineralization potential among the hPDL cells grown on LPS-coated scaffold environments (Fig. 4C).

Histone methyltransferases and demethylase affected PDL progenitor gene expression and cell function under inflammatory condition

Gene-specific changes in H3K4me3 and H3K27m3 enrichment under inflammatory condition suggest that H3K4me3 and H3K27me3 histone methyltransferases and/or demethylases may be involved in the regulation of periodontal progenitor gene expression and cell function. Here we have asked whether corresponding histone lysine methylation enzymes regulate trimethylation of the major active and repressive histone marks. Specifically, to determine whether SETD1 and/or KDM5B controls H3K4me3 levels or whether EZH2 and/or KDM6B controls H3K27me3 levels, we performed gene knockdown experiments using ON-TARGETplus small siRNAs specific for *SETD1*, *KDM5B*, *EZH2*, and *KDM6B* genes. Knockdown efficiency was 97% for *SETD1B*, 72% for *KDM5B*, 69% for *EZH2*, and 88% for *KDM6B* after 72 h of transfection. Knockdown of *EZH2* upregulated the expression of *COL3A1* (1.7-fold, $P < 0.05$) expression. Knockdown of *KDM6B* significantly reduced *COL1A1* (1.5-fold, $P < 0.05$) and *RUNX2* (1.3-fold, $P < 0.05$). These results indicate that osteogenic lineage and matrix proteins are regulated through modulating H3K27me3 levels. Knockdown of *SETD1B* downregulated *CCL5* (1.2-fold, $P < 0.05$), *DEFA4* (1.1-fold, $P < 0.05$), and *IL-1β* (1.2-fold, $P < 0.05$) expression. Overall, knockdown of *SETD1/KDM5B* or *EZH2/KDM6B* histone methylation enzymes resulted in highly unique changes in gene expression signatures (Fig. 5B). When applied in vitro, the specific reduction of *SETD1B* levels caused inhibition of LPS-induced PDLSCs migration (Fig. 5C, D). In contrast, a decrease in *EZH2* expression resulted in enhanced ALP activity of LPS-treated PDLSCs, whereas no effect on cell migration was recorded (Fig. 5C, D). In addition, in vitro knockdown of *KDM6B* inhibited ALP activity in human PDL cells (Fig. 5D). Together, these data demonstrate that changes in histone

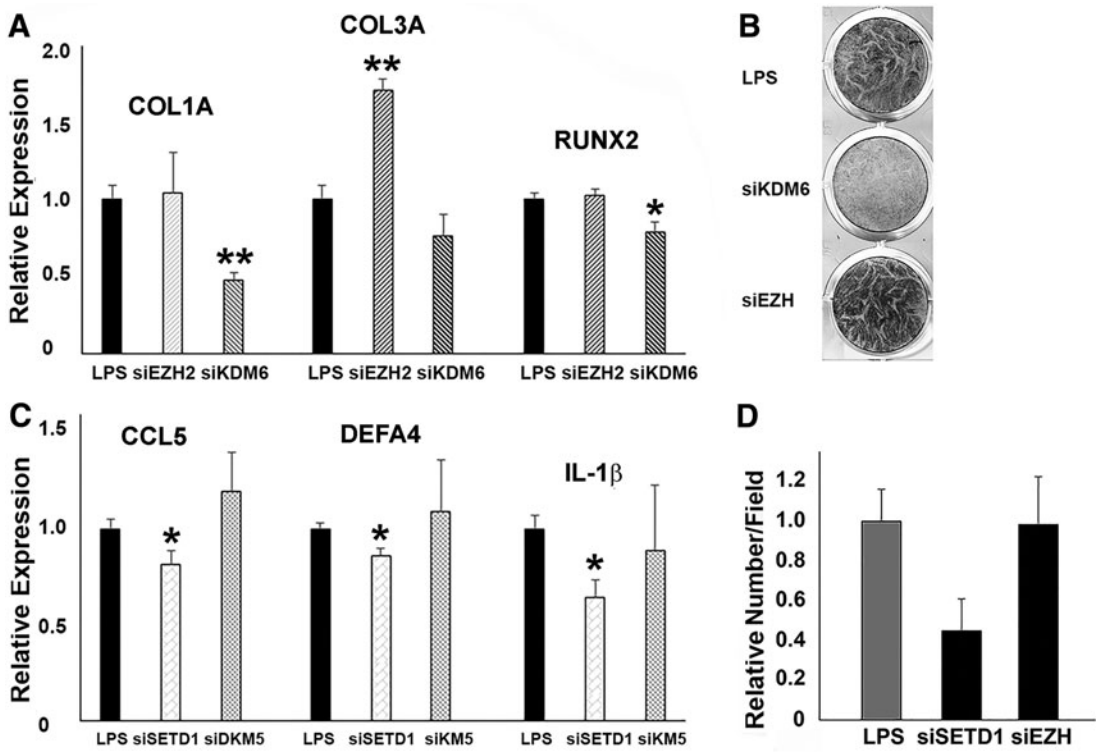

FIG. 5. Effects of *SETD1* or *EZH2* gene knockdown on cell function and gene expression. **(A)** Relative mRNA expression of *COL1A1*, *COL3A1*, and *RUNX2* genes after knockdown of *EZH2* and *KDM6B*. **(B)** ALP activity in PDLSCs after knockdown of *KDM6B* or *EZH2* gene. **(C)** Relative mRNA expression of *CCL5, IL-1β*, and *DEFA4* genes after knockdown of *SETD1B* and *KDM5B*. **(D)** Cell migration analysis of human PDLSCs challenged with LPS after knockdown of *SETD1B* or *EZH2*. PDLSC, periodontal ligament stem cell.

methylation and demethylation enzymes affect matrix and osteogenic lineage gene expression, inflammatory response gene, and periodontal progenitor function.

Discussion

This study was undertaken to provide a baseline assessment of the epigenetic regulation of the periodontal host response after exposure to bacterial cell wall toxins (LPS). Changes in histone methylation patterns in PDL progenitors were determined after LPS treatment in cell culture or after seeding of cells on LPS-coated and control scaffolds. In response to LPS, H3K27me3 enrichment increased on extracellular matrix and osteogenesis lineage gene promoters, whereas H3K4me3 enrichment increased on the promoters of inflammatory response genes. On a gene expression level, LPS treatment downregulated *COL1A1*, *COL3A1*, and *RUNX2* expression and upregulated *CCL*, *DEFA4*, and *IL-1β* gene expression. LPS also greatly affected PDLSC function, including a reduction in proliferation and differentiation potential and an increase in cell migration capacity. Together, these data suggest that LPS bacterial cell wall toxins affect gene expression in periodontal stem cells by modulating their histone methylation status, which in turn compromises periodontal stem cell function.

ChIP-on-chip analyses of hPDLSCs demonstrated high enrichment levels for the active H3K4me3 mark at *COL1A1*, *COL3A1*, and *RUNX2* gene promoters, whereas there were high occupancy levels for the repressive H3K27me3 marks at *DEFA4*, *CCL5*, and *IL-1β* gene promoters. These data provide a first glance at the extensive level of epigenetic control of periodontal lineage commitment and immune response. Similar histone methylation patterns at matrix and mineralization genes were also observed in other odontogenic progenitor cells including dental follicle and dental pulp stem cells [31]. The odontogenic progenitor-specific activation pathway of gene expression may allow these cells to produce nonmineralized or mineralized dental tissues during tooth development and regeneration based on environmental cues.

In hPDLSCs, LPS downregulated the expression of osteogenesis-related genes such as *COL1A1*, *COL3A1*, and *RUNX2* in PDL cells and decreased their osteogenic potential. Moreover, in subcutaneously implanted collagen sponges seeded with hPDLSCs, LPS increased cell infiltration, inhibited mineralization, and affected collagen matrix organization. The effects of LPS on periodontal matrix destruction are well-established [35,36]. In this study, we have correlated the effects of LPS on periodontal cell behavior and histone methyl mark enrichment on the promoters of osteogenic and inflammatory response genes. Specifically, we have discovered increased H3K27me3 occupancy on osteogenic and matrix gene promoters and increased H3K4me3 occupancy on inflammatory gene promoters upon LPS stimulation, providing a potential epigenetic mechanism by which these genes are regulated.

Our ChIP-on-chip of PDLSCs analysis indicated that in contrast to the active lysine methylation marks at extracellular matrix and mineralization gene promoters, inflammatory gene promoters were strongly repressed as evidenced by high levels of H3K9me3 and H3K27me3 enrichment. However, upon LPS challenge, the expression of inflammatory genes such as *DEFA4*, *CCL5*, and *IL-1β* was significantly increased, a trend echoed by a switch from repressive methyl marks to the active H3K4me3 marks on inflammatory gene promoters. On a cellular level, the effect of LPS on PDLSCs resulted in increased cell migration. Such behavior might be explained by the well-documented effects of proinflammatory cytokines and chemokines on proliferation, differentiation, and functions of stem cells and inflammatory cells [37–39]. Together, our data indicate that LPS regulates inflammation-related gene expression and cellular functions through histone methylation.

Our data demonstrated that histone methyltransferases were directly involved in the regulation of gene expression in PDLSCs under inflammatory conditions and their corresponding cell function. Recent studies indicate that LPS and proinflammatory cytokines have a direct inhibitory effect on osteoblastogenesis of mesenchymal progenitors including PDLSCs [18,34,40,41]. These inflammatory factors inhibit both the expression and function of the osteogenic master genes *RUNX2* and *OSX* [42]. In this study, *RUNX2* gene expression was downregulated in PDLSCs after LPS treatment. This inhibitory effect of LPS on *RUNX2* expression is associated with the increased enrichment of H3K27me3 on gene promoters (Figs. 2 and 3). The occupancy of H3K27me3 on the promoters of *RUNX2* and *OSX* genes seems to play a critical role during osteogenesis because both histone methyltransferase and demethylase for H3K27me3 regulate osteoblast differentiation. Especially the H3K27me3 methyltransferase EZH2 has been shown to inhibit osteogenic differentiation of MSCs, whereas the H3K27me3 demethylase Jmjd3 has an opposite effect and promotes osteogenic differentiation [20,43–45]. Other histone methylation modulating enzymes such as the H3K4 methyltransferases such as MLL1 [46], MLL4 [47] and COMPASS family members [48] are involved in the control of NF-κB-mediated gene expression by modulating H3K4 methylation states under inflammation conditions. Our study indicated that H3K27me3 labeling is absent or at low levels on the promoters of *RUNX2* and *COL1A1* and *COL3A1* in committed PDLSCs, indicative of the removal of H3K27me3 from genes that have been upregulated upon stem cell commitment [49]. Increase in the enrichment of H3K27me3 on the promoters of these genes under inflammatory conditions suggests that inflammatory environments influence gene expression and functions of MSCs through histone methylation and classic epigenetic enzymes.

Acknowledgment

Generous funding by NIDCR grants F30 DE 024352 to M.F. and 1R01 DE019463 to X.L. is gratefully acknowledged.

Author Disclosure Statement

No competing financial interests exist.

References

1. Gronthos S, K Mrozik, S Shi and PM Bartold. (2006). Ovine periodontal ligament stem cells: isolation, characterization, and differentiation potential. Calcif Tissue Int 79:310–317.
2. Roguljic H, BG Matthews, W Yang, H Cvija, M Mina and I Kalajzic. (2013). In vivo identification of periodontal progenitor cells. J Dent Res 92:709–715.
3. Dangaria SJ, Y Ito, C Walker, R Druzinsky, X Luan and TGH Diekwisch. (2009). Extracellular matrix-mediated differentiation of periodontal progenitor cells. Differentiation 78:79–90.
4. Dangaria SJ, Y Ito, X Luan and TGH Diekwisch. (2011). Differentiation of neural- crest-derived intermediate pluripotent progenitors into committed periodontal populations involves unique molecular signature changes, cohort shifts, and epigenetic modifications. Stem Cells Dev 20: 39–52.
5. Dangaria SJ, Y Ito, L Yin, G Valdré, X Luan and TGH Diekwisch. (2011). Apatite microtopographies instruct signaling tapestries for progenitor-driven new attachment of teeth. Tissue Eng Part A 17:279–290.
6. Shimono M, T Ishikawa, H Ishikawa, H Matsuzak, S Hashimoto, T Muramatsu, K Shima, K Matsuzaka and T Inoue. (2003). Regulatory mechanisms of periodontal regeneration. Microsc Res Tech 60:491–502.
7. Roeder E, BG Matthews and I Kalajzic. (2016). Visual reporters for study of the osteoblast lineage. Bone 92:189–195.
8. Graves DT. (1999). The potential role of chemokines and inflammatory cytokines in periodontal disease progression. Clin Infect Dis 28:482–490.
9. Chen SC, V Marino, S Gronthos and PM Bartold. (2006). Location of putative stem cells in human periodontal ligament. J Periodontal Res 41:547–553.
10. Zhu W and M Liang. (2015). Periodontal ligament stem cells: current status, concerns, and future prospects. Stem Cells Int 2015:1–11.
11. Liu N, S Shi, M Deng, L Tang, G Zhang, N Liu, B Din, W Liu, Y Liu, et al. (2011). High levels of β-catenin signaling reduce osteogenic differentiation of stem cells in inflammatory microenvironments through inhibition of the noncanonical Wnt pathway. J Bone Miner Res 26:2082–2095.
12. Park JC, JM Kim, IH Jung, JC Kim, SH Choi, KS Cho and CS Kim. (2011). Isolation and characterization of human periodontal ligament (PDL) stem cells (PDLSCs) from the inflamed PDL tissue: in vitro and in vivo evaluations: stem cells from inflamed PDL. J Clin Periodontol 38:721–731.
13. Zheng W, S Wang, J Wang and F Jin. (2015). Periodontitis promotes the proliferation and suppresses the differentiation potential of human periodontal ligament stem cells. Int J Mol Med 36:915–922.
14. Jain S and RP Darveau. (2010). Contribution of Porphyromonas gingivalis lipopolysaccharide to periodontitis: *P. gingivalis* lipopolysaccharide in periodontitis. Periodontol 2000 54:53–70.

15. Darveau RP. (2010). Periodontitis: a polymicrobial disruption of host homeostasis. Nat Rev Microbiol 8:481–490.
16. Yamaji Y, T Kubota, K Sasaguri, S Sato, Y Suzuki, Ku H mada and T Umemoto. (1995). Inflammatory cytokine gene expression in human periodontal ligament fibroblasts stimulated with bacterial lipopolysaccharides. Infect Immun 63:6.
17. Nebel D, D Jönsson, O Norderyd, G Bratthall and BO Nilsson. (2010). Differential regulation of chemokine expression by estrogen in human periodontal ligament cells: chemokines and estrogen in PDL cells. J Periodontal Res 45:796–802.
18. Kukolj T, D Trivanović, IO Djordjević, S Mojsilović, J Krstić, OH bradović, S Janković, JF Santibanez, A Jauković, et al. (2018). Lipopolysaccharide can modify differentiation and immunomodulatory potential of periodontal ligament stem cells via ERK1,2 signaling. J Cell Physiol 233:447–462.
19. Kawai T and S Akira. (2007). Signaling to NF-κB by toll-like receptors. Trends Mol Med 13:460–469.
20. Ye L, Z Fan, B Yu, J Chang, K Al Hezaim, X Zhou, NH Park and CY Wang. (2012). Histone demethylases KDM4B and KDM6B promotes osteogenic differentiation of human MSCs. Cell Stem Cell 11:50–61.
21. Xu J, B Yu, C Hong and CY Wang. (2013). KDM6B epigenetically regulates odontogenic differentiation of dental mesenchymal stem cells. Int J Oral Sci 5:200–205.
22. Rojas A, AR guilar, B Henriquez, JB Lian, JL Stein, GS Stein, AJ van Wijnen, B van Zundert, ML Allende, et al. (2015). Epigenetic control of the bone-master runx2 gene during osteoblast-lineage commitment by the histone demethylase JARID1B/KDM5B. J Biol Chem 290:28329–28342.
23. Rui Y, L Xu, R Chen, T Zhang, S Lin, Y Hou, Y Liu, F Meng, Z Liu, et al. (2015). Epigenetic memory gained by priming with osteogenic induction medium improves osteogenesis and other properties of mesenchymal stem cells. Sci Rep 5:11056.
24. Rosenfeld MG. (2006). Sensors and signals: acoactivator/corepressor/epigenetic code for integrating signal-dependent programs of transcriptional response. Genes Dev 20:1405–1428.
25. Yu H, S Zhu, B Zhou, H Xue and DJ Han. (2008). Inferring causal relationships among different histone modifications and gene expression. Genome Res 18:1314–1324.
26. Cui K, C Zan, TY Roh, DE Schones, RW Childs, W Peng and K Zhao. (2009). Chromatin signatures in multipotent human hematopoietic stem cells indicate the fate of bivalent genes during differentiation. Cell Stem Cell 4: 80–93.
27. Bernstein BE, TS Mikkelsen, X Xie, M Kamal, DJ Huebert, J Cuff, B Fry, A Meissner, M Wernig, et al. (2006). A Bivalent chromatin structure marks key developmental genes in embryonic stem cells. Cell 125:315–326.
28. Zhao XD, X Han, JL Chew, J Liu, KP Chiu, A Choo, YL Orlov, WK Sung, A Shahab, et al. (2007). Whole-genome mapping of histone H3 Lys4 and 27 trimethylations reveals distinct genomic compartments in human embryonic stem cells. Cell Stem Cell 1:286–298.
29. Pan G, S Tian, J Nie, C Yang, V Ruotti, H Wei, GA Jonsdottir and St R ewart, JA Thomson. (2007). Whole-genome analysis of histone H3 Lysine 4 and Lysine 27 methylation in human embryonic stem cells. Cell Stem Cell 1:299–312.
30. Leu YW, Huang THM and Hsiao SH. (2013). Epigenetic reprogramming of mesenchymal stem cells. In: *Epigenetic Alterations in Oncogenesis*. Karpf AR, ed. Springer New York, New York, NY, 754, pp 195–211.
31. Gopinathan G, A Kolokythas, X Luan and TGH Diekwisch. (2013). Epigenetic marks define the lineage and differentiation potential of two distinct neural crest-derived intermediate odontogenic progenitor populations. Stem Cells Dev 22:1763–1778.
32. Bayarsaihan D. (2011). Epigenetic mechanisms in inflammation. J Dent Res 90:9–17.
33. Eslani M, A Movahedan, N Afsharkhamseh, H Sroussi and AR Djalilian. (2014). The role of Toll-Like receptor 4 in corneal epithelial wound healing. Investig Opthalmol Vis Sci 55:6108.
34. Pan S, S Dangaria, G Gopinathan, X Yan, X Lu, A Kolokythas, Y Niu and X Luan. (2013). SCF promotes dental pulp progenitor migration, neovascularization, and collagen remodeling—potential applications as a homing factor in dental pulp regeneration. Stem Cell Rev Rep 9:655–667.
35. Page RC. (1991). The role of inflammatory mediators in the pathogenesis of periodontal disease. J Periodontal Res 26: 230–242.
36. Ijuhin N, M Miyauchi, H Ito, T Takata, I Ogawa and H Nikai. (1992). Enhanced collagen phagocytosis by rat molar periodontal fibroblasts after topical application of lipopolysaccharide—ultrastructural observations and morphometric analysis. J Periodontal Res 27:167–175.
37. Pietras EM. (2017). Inflammation: a key regulator of hematopoietic stem cell fate in health and disease. Blood 130: 1693–1698.
38. Crop MJ, CC Baan, SS Korevaar, JN Ijzermans, M Pescatori, AP Stubbs, WF van Ijcken, MH Dahlke, E Eggenhofer, et al. (2010). Inflammatory conditions affect gene expression and function of human adipose tissue-derived mesenchymal stem cells: effect of inflammatory conditions on ASC. Clin Exp Immunol 162:474–486.
39. Doles J, M Storer, L Cozzuto, G Roma and WM Keyes. (2012). Age-associated inflammation inhibits epidermal M stem cell function. Genes Dev 26:2144–2153.
40. Luan X, X Zhou, J Trombetta-eSilva, M Francis, AK Gaharwar, P Atsawasuwan and TGH Diekwisch. (2017). MicroRNAs and periodontal homeostasis. J Dent Res 96: 491–500.
41. Zhou X, X Luan, Z Chen, M Francis, G Gopinathan, W Li, X Lu, S Li, C Wu and TG Diekwisch. (2016). MicroRNA-138 inhibits periodontal progenitor differentiation under inflammatory conditions. J Dent Res 95:230–237.
42. Gilbert L, X He, P Farmer, J Rubin, H Drissi, AJ van Wijnen, JB Lian, GS Stein and MS Nanes. (2002). Expression of the osteoblast differentiation factor RUNX2 (Cbfa1/AML3/Pebp2αA) is inhibited by tumor necrosis factor-α. J Biol Chem 277:2695–2701.
43. Dudakovic A, ET Camilleri, F Xu, SM Riester, MME cGee-Lawrence, EW Bradley, CR Paradise, EA Lewallen, TR haler, et al. (2015). Epigenetic control of skeletal development by the histone methyltransferase Ezh2. J Biol Chem 290:27604–27617.
44. Wei G, L Wei, J Zhu, C Zang, J Hu-Li, Z Yao, K Cui, Y Kanno, TY Roh, et al. 2009. Global mapping of H3K4me3 and H3K27me3 reveals specificity and plasticity in lineage fate determination of differentiating CD4+ T cells. Immunity30:155–167.

45. Yang D, H Okamura, Y Nakashima and T Haneji. (2013). Histone demethylase Jmjd3 regulates osteoblast differentiation via transcription factors Runx2 and Osterix. J Biol Chem 288:33530–33541.
46. Wang X, K Zhu, S Li, Y Liao, R Du, X Zhang, HB Shu, AY Guo, Li L, et al. (2012). MLL1, a H3K4 methyltransferase, regulates the TNFα-stimulated activation of genes downstream of NF-κB. J Cell Sci 125:4058–4066.
47. Austenaa L, I Barozzi, A Chronowska, A Termanini, R Ostuni, E Prosperini, AF Stewart, G Testa and G Natoli. (2012). The histone methyltransferase Wbp7 controls macrophage function through GPI glycolipid anchor synthesis. Immunity 36:572–585.
48. Yu L, X Weng, P Liang, Dai X, X Wu, H Xu, M Fang, F Fang and Y Xu. (2014). MRTF-A mediates LPS-induced pro-inflammatory transcription by interacting with the COMPASS complex. J Cell Sci 127:4645–4657.
49. Wu Q, B Yang, K Hu, C Cao, Y Man and P Wang. (2017). Deriving osteogenic cells from induced pluripotent stem cells for bone tissue engineering. Tissue Eng Part B Rev 23:1–8.

Address correspondence to:
Prof. Xianghong Luan
Department of Periodontics
Center for Craniofacial Research and Diagnosis
Texas A&M College of Dentistry
3302 Gaston Avenue
Dallas, TX 75246

E-mail: luan@tamu.edu

Received for publication June 16, 2019
Accepted after revision June 18, 2019
Prepublished on Liebert Instant Online June 20, 2019